



Electrochemical recovery of silver from cyanide leaching solutions

V. REYES CRUZ, M.T. OROPEZA, I. GONZÁLEZ* and C. PONCE-DE-LEÓN

Universidad Autónoma Metropolitana-Izt, Departamento de Química, Apdo. Postal 55-534, CP 09340 México DF, México

(*author for correspondence, fax +52 55 5804-4666, e-mail: igm@xanum.uam.mx)

Received 27 July 2001; accepted in revised form 29 January 2002

Key words: copper cyanide complexes, cross-flow reactor, cyanide leaching, electrochemical recovery, RVC electrode, silver cyanide complexes

Abstract

In the hydrometallurgy industry cyanide solutions are the most common leaching baths used during the extraction of metals such as silver and gold. After extraction, the solution containing various cyanide species, and usually copper cyanide, has a higher concentration than the gold and silver complexes. Higher concentration of copper species may interfere during the selective recovery of precious metals. This work presents a study of the selective recovery of silver from leaching solutions mimicking those used in industry. Chemical speciation and cyclic voltammetry studies showed that copper reduction occurs at more negative potentials than silver in the cyanide leaching solutions. The cyclic voltammetry of cyanide solutions on a vitreous carbon electrode showed that copper cyanide ions modify the interface properties, lowering the overpotential required for silver reduction. A macroelectrolysis study of a simulated leaching solution (10^{-4} M Ag(I), 0.1 M Cu(I) in 0.5 M CN^- at pH 10), was carried out in a filter press electrochemical reactor (ElectroCell AB) with a reticulated vitreous carbon electrode (RVC), nominally having 45 pores per inch and a flow rate of $5 \text{ cm}^3 \text{ s}^{-1}$ at 25°C . The study showed that the high copper concentration does not interfere in the selective deposition of silver.

1. Introduction

Among hydrometallurgical processes, cyanide leaching followed by solid–liquid separations, is the most common for the treatment of gold and silver ores [1, 2]. The most important minerals in the metallurgical industry are those that contain high concentrations of gold (100 g ton^{-1}) and silver (1200 g ton^{-1}). However, some minerals have lower concentration of the precious metals with high concentration of copper, which can be over a hundred times the concentration of gold and silver. Generally, cyanide metallic species from raw material are dissolved in aqueous medium after leaching. Regarding the concentration criteria, it might be expected that the higher copper concentration might interfere with the selective recovery of precious metals [3].

After leaching, the solution commonly follows two lines: one for the concentrated solution and the other for the dilute solution. Each line is processed to remove the metallic species, such as copper, using ionic exchange resins or activated carbon columns, thus giving a concentrated solution of precious metals. The next stage is the recovery and refining in which two traditional methods are used: cementation and electrolysis [2, 3].

The former process has only been used in concentrated solutions with conventional electrochemical reactors (plane electrodes), since in dilute solutions it has low current efficiency due to mass transfer limitation of the electroactive species [3, 4]. Several works have shown that the use of porous electrodes eliminates this disadvantage by increasing the specific area and thus the mass transfer [5–10].

Some authors have studied the reduction of precious metals at concentrations within the range 20–1000 ppm in cyanide solutions using porous electrodes (e.g., [11]). However, the recovery of precious metals at very low concentrations from cyanide leaching solutions (about 1–10 ppm) has received little attention [12].

Today, innovations in electrochemical reactor design (such as turbulence promotion and high specific area) have allowed the electrolytic process to be considered as an alternative for silver and gold recovery from dilute solutions [13–22]. This approach allows the selective recovery of silver from cyanide solutions containing higher concentrations of copper.

This work presents chemical speciation and cyclic voltammetric studies of a solution with similar characteristics to leaching cyanide solutions, containing silver and copper. The purpose is to determine how the

selective recovery of Ag(I) in cyanide solution can be affected by high concentrations of Cu(I). After establishing the potential range at which only silver must be reduced, the macroelectrolysis of the leaching solution (containing silver and copper) was carried out in a flow cell in batch recirculation.

2. Experimental details

A 100-ml Pyrex cell with a three-electrode system and nitrogen inlet was used in the voltammetric study. The working electrode was a vitreous carbon disc with geometric area of 0.07 cm². The electrode surface was polished with 0.3 μm alumina powder/water and rinsed with deionised water followed by treatment in an ultrasonic bath for 5 min to remove traces of alumina and grease and a final rinse with deionized water. The reference and counter electrodes were saturated calomel and a graphite rod, respectively. The solutions were: (a) cyanide solution (0.5 M KCN); (b) cyanide solution with Ag(I) (10⁻⁴ M AgNO₃ and 0.5 M KCN); (c) cyanide solution with Cu(I) (0.1 M CuCN and 0.5 M KCN); and (d) cyanide solution with Ag(I) and Cu(I) (0.1 M CuCN, 10⁻⁴ M AgNO₃ and 0.5 M KCN).

All solutions were prepared with deionized water 18 mΩ⁻¹ cm⁻¹ and analytical grade reagents. The pH was held constant at 10 and the solutions were deoxygenated with nitrogen for ten minutes prior to the cyclic voltammetric experiments. A flux of nitrogen blanketed the surface of the solution during the experiments without disturbing the electrolyte.

The macroelectrolysis for the selective reduction of Ag(I) in the presence of high concentrations of Cu(I) (solution (d)) was carried out using a filter press electrochemical reactor (ElectroCell AB). A full description of this cell has been given elsewhere [17]. A cationic membrane NAFION NX550 separated the anodic and cathodic compartments. The cathode was a reticulated vitreous carbon (RVC) electrode with 45 pores per inch (ppi), filling a volume of 9.24 cm³ (Electrosynthesis, Co.). Copper plates glued by conductive carbon paste made the electrical contact with the RVC electrode. The anode was a graphite plate.

The electrolyte was recirculated through the cell using a twin head peristaltic pump (Cole Palmer) with velocity (5 cm³ s⁻¹ at 25 °C). A potentiostat (EG&G model PAR 273) and M270 software were used in the voltammetric and macroelectrolysis experiments. The determination of the total Ag(I) and Cu(I) concentrations was carried out by atomic absorption spectroscopy (AAS). Surface characterizations were obtained by X-ray diffraction (XDR) using a Siemens D500 diffractometer with CuKα radiation. Scanning electron microscopy (SEM) was used to observe the metal morphology. The study was carried out using a SEM Carl Zeis DSM 940A microscope coupled to a WDX detector.

3. Results and discussion

3.1. Chemical speciation study

A chemical speciation study was performed to establish the nature of the electroactive species of silver and copper in cyanide solutions. Figure 1 shows the overlapped Pourbaix type diagrams for Ag and Cu species. These diagrams were constructed using data for soluble and insoluble species of Ag and Cu [23–25], and taking into account the conditions of the leaching solution for minerals ($p\text{CN}' = -\log [\text{CN}'] = 0.222$, $p\text{Ag}' = -\log [\text{Ag}'(\text{I})] = 4$, and $p\text{Cu}'(\text{I}) = -\log [\text{Cu}'(\text{I})] = 1$) using the methodology proposed by Rojas et al. [26, 27]. Under these conditions, there are four and two generalized species of copper and silver, respectively. It is important to note that the interaction between copper and silver alloy and intermetallic deposit are not considered in these diagrams.

The solid lines in Figure 1 represent the conditional potential change of the system M'(I)/M(0) with pH. The dotted lines represent the limit of the pH range where the metal ion species (Ag(I) or Cu(I)) predominates (high molar fraction), with respect to the other cyanide species of the same metallic ion (generalized chemical species). In the case of copper, the dotted line at pH 3.8 corresponds to the solubility limit for CuCN_(s).

From Figure 1, it is possible to calculate the conditional redox equilibrium potential E''' , associated with the redox reactions Ag'(I)/Ag(0) and Cu'(I)/Cu(0) at pH 10, $p\text{CN}' = 0.22$, $p\text{Ag}' = 4$ and $p\text{Cu}' = 1$:

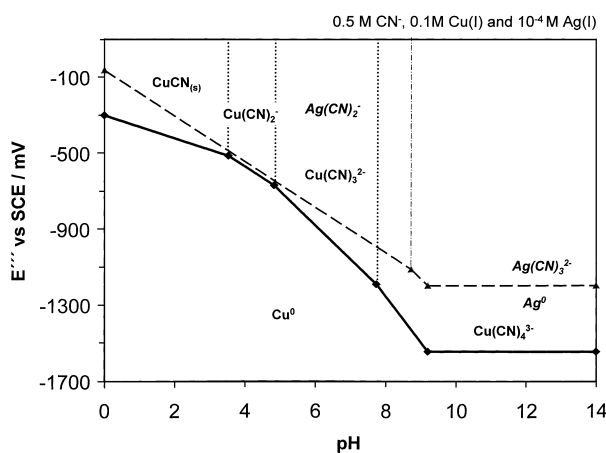
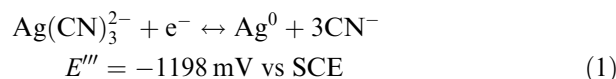
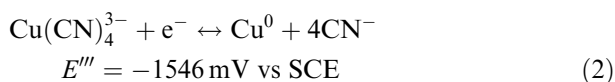


Fig. 1. Pourbaix-type diagrams of soluble and insoluble chemical species involved in the redox couples: Ag'(I)/Ag(0) (---) and Cu'(I)/Cu(0) (—). Diagrams were constructed independently with thermodynamical data from the literature considering the following concentrations as nonvariable: 10⁻⁴ M Ag'(I) and 0.1 M Cu'(I) in 0.5 M CN⁻. The concentration of these chemical species represents the composition found in cyanide leaching solutions.



Thus, the selective reduction of silver is thermodynamically possible in this leaching solution.

3.2. Voltammetric study

A voltammetric study of the cyanide solutions with and without metallic ions was carried out on a planar vitreous carbon electrode within the range 100 to -1800 mV vs SCE.

Figure 2 shows a voltammetric comparison of the following solutions: cyanide solution free from metallic ions (curve (a)), cyanide solution with Ag(I) (curve (b)), cyanide solution with Cu(I) (curve (c)) and cyanide solution with both Cu(I) and Ag(I) (curve (d)). In Figure 2, (curve (a)), the capacitive current density has been attributed to the cyanide species adsorbed onto the electrode surface [28–30]. It is important to note that the electrode capacitance was not evaluated and just a qualitative interpretation will be presented. Towards negative potentials, a current density increase due to water reduction, was observed. In solutions containing

Ag(I) (inset Figure 2, curve (b)), the same reaction occurs, but at less negative potentials, while there is no difference in the current density before the water reduction between this case and the cyanide solution case. The increase in current density is a consequence of the simultaneous reduction of silver ions and water.

Since the concentration of Ag(I) is low, its reduction (Equation 1) current density was masked by the capacitive current and by water reduction. However, the oxidation peak at -712 mV vs SCE, shows that metallic silver has been deposited onto the vitreous carbon electrode during the forward scan (Figure 2, curve (b)). The capacitive current density in the cyanide solutions was not modified by the presence of Ag(I) (inset Figure 2, curves (a) and (b)). This was attributed to the fact that silver reduction does not involve adsorbed Ag(I) species [31, 32].

The cyanide solution containing Cu(I) (solution (c)) shows a different voltammetric response (Figure 2, curve (c)), shifting the hydrogen evolution negatively and changing the capacitive current density. The latter effect was due to the adsorption of copper cyanide complex ions onto the vitreous carbon surface [28, 29]; these compete with the adsorbed cyanide species [28–30]. On the other hand, the reduction of copper should occur at potentials more negative than negative switching potentials and where neither the reduction nor the oxidation of copper is observed in Figure 2.

The presence of Cu(I) in the Ag(I) cyanide solution (solution (d)) shifts the hydrogen evolution to more negative potentials with respect to the Ag(I) cyanide solution (inset Figure 2, curves (d) and (b), respectively). Also, the effect of Cu(I) on the voltammetric behaviour is very similar regarding the capacitive current densities either with or without silver (Figure 2, curves (d) and (c), respectively) up to a potential of -1200 mV vs SCE. This behaviour suggests that silver reduction does not require adsorbed species on the electrode surface. Furthermore, Cu(I) allows both the reduction process of Ag(I) (Equation 1) from -1200 to -1500 mV vs SCE (reduction wave I, inset Figure 2) and the oxidation peak of Ag(0) to Ag(I) at -675 mV vs SCE to be distinguished. The presence of Cu(I) in cyanide solutions seems to increase the current density in the silver oxidation peak (inset Figure 2). However, the peak was shifted toward less negative potentials (-675 mV vs SCE) than those observed in the absence of copper (-712 mV vs SCE), possibly indicating a codeposition of Cu/Ag (see below) or higher amounts of deposited silver.

The competition between the different adsorbed species onto the vitreous carbon causes a modification of the voltammetric response. In this work, we associate this behavior with the modification of the capacitive current densities. A more detailed study of these capacitive currents could be done; however, we have discussed our results in the light of assumptions previously reported [28–32].

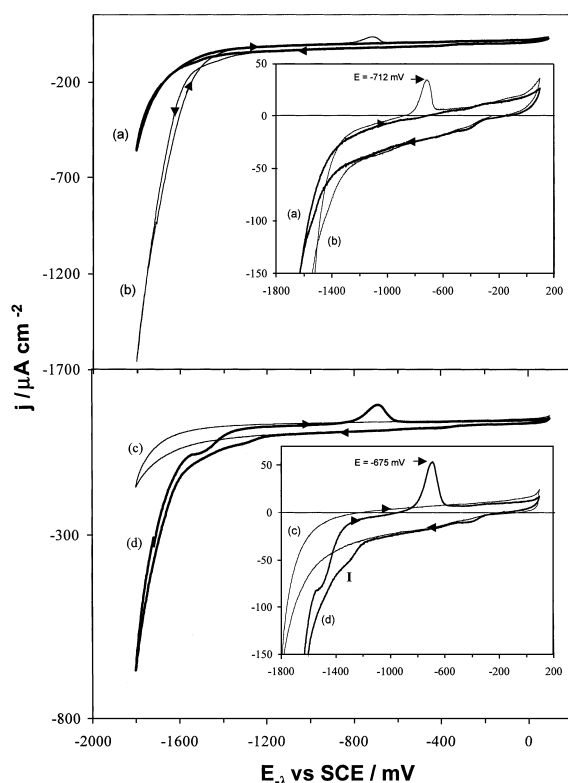


Fig. 2. Typical cyclic voltammograms obtained from an aqueous solution containing 0.5 M CN^- at pH 10, on a vitreous carbon disc (0.07 cm^2), at 25 mVs^{-1} . Curves show influence of different ions: (a) free of metallic ions, (b) $10^{-4} \text{ M Ag}(\text{CN})_3^{2-}$, (c) $0.1 \text{ M Cu}(\text{CN})_4^{3-}$ and (d) $10^{-4} \text{ M Ag}(\text{CN})_3^{2-}$ and $0.1 \text{ M Cu}(\text{CN})_4^{3-}$. Insets show voltammetric responses at low current densities. Silver oxidation peak potentials are indicated.

The aforementioned analysis shows that Cu(I) modifies the interface properties and allows the reduction and the oxidation processes of silver to be distinguished. However, it is necessary to identify the potential range in which Ag(I) may be selectively reduced in solutions containing high concentrations of copper. This can be done by a voltammetric study changing the negative switching potential ($E_{-λ}$).

3.3. Influence of the negative switching potential ($E_{-λ}$)

Figure 3 shows the voltammograms obtained at different negative switching potentials ($E_{-λ}$) during the reduction of silver cyanide solutions in the absence and presence of Cu(I).

Figure 3(a), shows that the silver oxidation peak was detected only when $E_{-λ} < -1600$ mV vs SCE (Figure 3(a), curves (ii)–(iv)) and the reduction process was not seen during the forward potential scans. The current peak for silver oxidation increased as $E_{-λ}$ was progressively taken to more negative values; meanwhile, the potential peak shifted towards less negative potentials (from -716 to -696 mV vs SCE). This behaviour is typical of an oxidation process from a newly deposited metal [33].

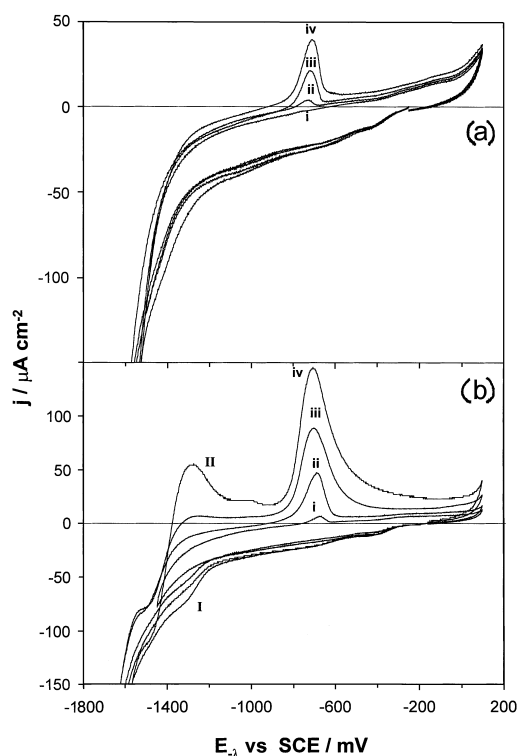


Fig. 3. Partial view of typical cyclic voltammograms obtained from an aqueous solution containing 10^{-4} M $\text{Ag}(\text{CN})_3^{2-}$ in 0.5 M CN^- at pH 10, on a vitreous carbon disc (0.07 cm 2) at 25 mV s $^{-1}$. Voltammograms were obtained at different negative switching potentials ($E_{-λ}$): (a) without Cu(I), (i) $E_{-λ} = -1500$ mV, (ii) $E_{-λ} = -1600$ mV, (iii) $E_{-λ} = -1700$ mV, (iv) $E_{-λ} = -2000$ mV; (b) with 0.1 M $\text{Cu}(\text{CN})_4^{3-}$, (i) $E_{-λ} = -1400$ mV, (ii) $E_{-λ} = -1600$ mV, (iii) $E_{-λ} = -2200$ mV, (iv) $E_{-λ} = -2500$ mV.

In the cyanide solution containing Cu(I) and Ag(I) (Figure 3(b)) it is possible to distinguish the reduction process I of Ag(I). This process was detected from $E_{-λ} = -1400$ mV vs SCE (Figure 3(b), curve (i)). As $E_{-λ}$ was taken to more negative values (-1400 mV $< E_{-λ} < -1900$ mV vs SCE), the oxidation current peak and its corresponding potential shifted to more negative values (from -660 to -686 mV). (Figure 3(b), curves (i)–(iii)), indicating silver deposition (Equation 1). From -1900 mV $\leq E_{-λ} < -2000$ mV vs SCE, the oxidation peak shape changes, suggesting the formation of a codeposit. On the other hand, the appearance of an oxidation peak II at -1300 mV vs SCE only occurs at $E_{-λ} \leq -2200$ mV vs SCE (Figure 3(b), curve (iv)) and is attributed to the conversion of Cu(0) to Cu(I) (Equation 2). This response was similar to that obtained from a cyanide solution containing only Cu(I), when $E_{-λ}$ reached -2200 mV vs SCE, as shown in Figure 4.

To identify the potential range in which copper and silver were selectively deposited, a quantitative study of the voltammetric curves was carried out. The associated charge of the silver oxidation peak (Q_a) for systems with and without copper, were evaluated and plotted as a function of the negative switching potential ($E_{-λ}$). Figure 5 shows Q_a vs $E_{-λ}$ for a silver cyanide solution (case (a)) and for a solution containing both silver and copper cyanides (case (b)). The slope corresponding to the Ag(I) system ($m = -0.51$ $\mu\text{C cm}^{-2} \text{mV}^{-1}$), is very similar to that of case (b) at less negative $E_{-λ}$ ($m = -0.56$ $\mu\text{C cm}^{-2} \text{mV}^{-1}$), indicating that only silver deposition occurs in both processes. At more negative $E_{-λ}$, silver cyanide solution slope, m , (Figure 5, case (a)) decreases due to the simultaneous reduction of water and silver.

Figure 5 shows that silver reduction was modified by the presence of Cu(I). The slope does not change ($m = -0.56$ $\mu\text{C cm}^{-2} \text{mV}^{-1}$) until $E_{-λ} = -2000$ mV vs SCE and after this point, a large change occurs ($m = -1.32$ $\mu\text{C cm}^{-2} \text{mV}^{-1}$), which may be attributed

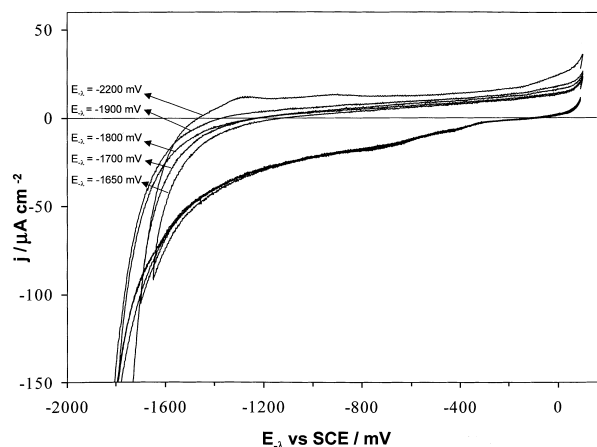


Fig. 4. Typical cyclic voltammograms obtained from an aqueous solution containing 0.1 M $\text{Cu}(\text{CN})_4^{3-}$, 0.5 M CN^- at pH 10, on a carbon vitreous disc (0.07 cm 2) at 25 mV s $^{-1}$. Voltammograms were obtained at different negative switching potentials ($E_{-λ}$) (as shown).

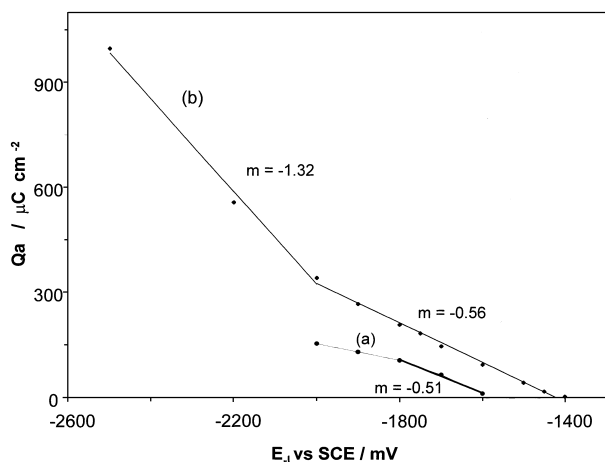


Fig. 5. Oxidation charge (Q_a) associated to the silver peak dissolution as a function of negative switching potential ($E_{-\lambda}$) from voltammograms of Figure 3, obtained from an aqueous solution containing 10^{-4} M $\text{Ag}(\text{CN})_3^{2-}$ in 0.5 M CN^- at pH 10, on a vitreous carbon disc (0.07 cm 2) at 25 mV s $^{-1}$. Influence of Cu(I) in solution (a) without Cu(I), (b) in presence of 0.1 M $\text{Cu}(\text{CN})_4^{3-}$. Slopes m are indicated.

to the codeposition of Cu/Ag, despite the absence of an additional oxidation peak. Thus, the oxidation of copper in the codeposit is equal, or very similar, to that of silver, since it is not possible to differentiate between them. The same slope changes were observed in a similar experiment with a cyanide solution containing 10^{-4} M Au(I), 10^{-4} M Ag and 10^{-1} M Cu(I) when different codeposits appeared [34].

The voltammetric study shows that due to the presence of Cu(I), the deposition of silver is energetically more efficient; the charges calculated for silver cyanide solutions containing Cu(I) (Figure 5, case (b)) are higher than those with only silver cyanide (Figure 5, case (a)) at the same $E_{-\lambda}$ values. The presence of Cu(I) makes the free cyanide concentration lower, thus changing the reaction mechanism of silver [35]. The electrochemical reaction proceeds by the discharge of silver complexes with less cyanide ligands, making its reduction easier.

The voltammetric study established that silver reduction under the above mentioned conditions (Figure 5) was within the range -1400 to -2000 mV vs SCE without reduction of Cu(I) onto a vitreous carbon surface. It is important to mention that this surface is very similar to the reticulated vitreous carbon [36] and it is assumed that the same interfacial conditions reached in the voltammetric study may be achieved in a reticulated vitreous carbon electrode for metal deposition.

3.4. Macroelectrolysis study

Once the potential range of Ag(I) deposition in the presence of Cu(I) was established, and taking into account that the concentration of silver was low (the capacitive currents masked the faradaic currents), a macroelectrolysis of 10^{-4} M AgCN_3^{2-} and 0.1 M $\text{Cu}(\text{CN})_4^{3-}$ in 0.5 M CN^- at pH 10 was carried out in a batch electrochemical reactor with recirculation. A

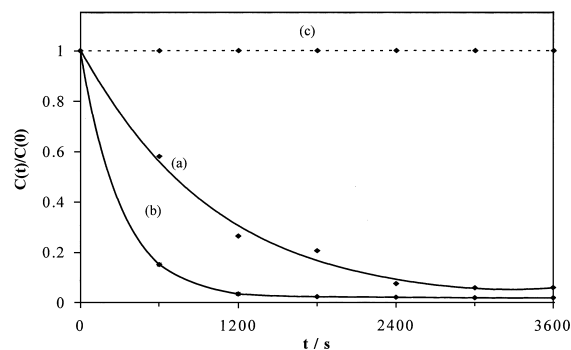


Fig. 6. Change of normalized concentration (ratio of concentration at any time ($C(t)$) and initial concentration ($C(t = 0)$) of cyanide metallic species in the catholyte compartment with time during the electrolysis of solution containing: 10^{-4} M $\text{Ag}(\text{CN})_3^{2-}$, and 0.1 M $\text{Cu}(\text{CN})_4^{3-}$ in 0.5 M CN^- at pH 10. Concentration profile of Ag(I) at different electrolysis potentials: (a) -1300 mV and (b) -1500 mV vs SCE. Curve (c) shows concentration profile of Cu(I) at both electrolysis potentials. Macroelectrolysis was carried out in a batch type electrochemical reactor using a RVC of 45 ppi at a flow rate of 5 cm 3 s $^{-1}$.

constant potential electrolysis was imposed on a RVC electrode for more than 1 h at a flow rate of 5 cm 3 s $^{-1}$. During macroelectrolysis, samples from the catholyte were taken at regular intervals. Determination of the total concentration of Cu(I) and Ag(I) was carried out by atomic absorption spectroscopy (AAS). Figure 6 shows the change in Ag(I) and Cu(I) concentrations normalized as $C(t)/C(0)$ as a function of time. Silver depletion was observed when potentials of -1300 mV and -1500 mV vs SCE were, respectively, imposed (Figure 6, curves (a) and (b)). However, as expected, silver depletion at -1500 mV vs SCE was faster. The quantitative analysis of the batch decay kinetics beyond the scope of this work. On the other hand, Figure 6, curve (c) shows that the Cu(I) concentration was independent of time at the mentioned potentials, indicating that the electroactive species $\text{Cu}(\text{CN})_4^{3-}$ remains constant during electrolysis. Despite the geometrical and possible surface differences between a planar vitreous carbon and a porous vitreous carbon surface the results obtained show that they have the same electrochemical behaviour.

To verify the presence of metallic silver on the electrode surface after electrolysis, a scanning electron microscopy followed by X-ray analysis was performed on the RVC electrode. Figure 7 shows three images at different resolutions of the RVC electrode after macroelectrolysis of the silver and copper cyanide solution at a potential of -1500 mV vs SCE. The fine white dendrites on the RVC surface correspond to a silver deposit. The spectral lines of the X-ray analysis shows only the presence of silver, indicating that there is no copper on the deposit. Thus, in cyanide baths it is possible to reduce Ag(I) leaving Cu(I) in solution, using a recirculation batch reactor, despite the difference of two orders of magnitude between the metal ionic concentrations.

The silver reduction in the electrochemical batch reactor presented here is a preliminary study showing that silver can be selectively reduced on a vitreous

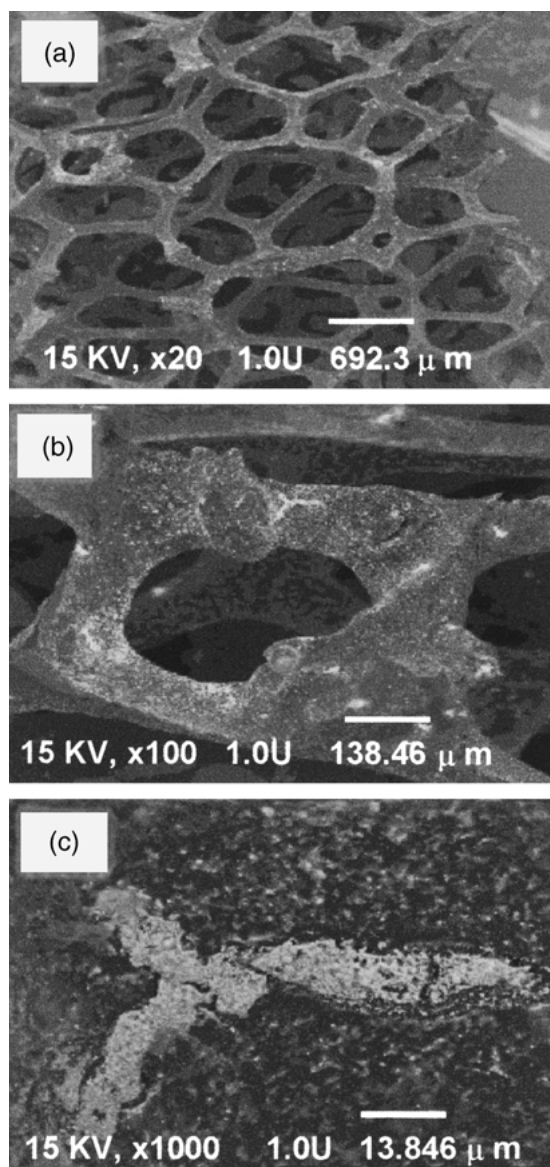


Fig. 7. Scanning electron microscopy (SEM) image of 45 ppi of the RVC electrode after the electrolysis of aqueous solution containing 10^{-4} M $\text{Ag}(\text{CN})_2^-$ and 0.1 M $\text{Cu}(\text{CN})_4^{3-}$ in 0.5 M CN^- , pH 10 at -1500 mV vs SCE. Magnifications: (a) $\times 20$, (b) $\times 100$, (c) $\times 1000$.

carbon surface. However, further studies such as current efficiency, mass transport and space-time yield and batch kinetics are necessary to design an efficient electrochemical reactor for the recovery of precious metal from leaching process solutions.

4. Conclusions

The presence of Cu(I) favours the silver recovery: enhances the silver reduction/oxidation processes and diminishes the potential for silver deposition. The reaction mechanism of silver deposition was modified by the presence of Cu(I), which leaves less free cyanide species in solution. A well defined potential range for Ag(I) deposition in the presence of high Cu(I) concentrations was established.

Silver at low concentrations (10^{-4} M) was recovered without reducing Cu(I), despite the concentration differences. This result agrees with the cyclic voltammetric results indicating a homogeneous potential distribution in the reticulated vitreous carbon.

The detected metallic silver (SEM images) in the RVC electrode confirms the selective deposition of silver. However, these are preliminary studies and further work is necessary in order to optimize reactor performance.

Acknowledgements

The authors express their gratitude to Conacyt (project number 32539-T) and Servicios Industriales Peñoles (Monterrey, México) for funding this work. V. Reyes-Cruz thanks Conacyt and Servicios Industriales Peñoles (Monterrey México) for his PhD scholarship. The authors also thank M. Teresa Ramírez for her help in the construction of the Pourbaix diagrams.

References

1. G.A. Kordosky, J.M. Sierakosky, M.J. Virnig and P.L. Mattison, *Hydrometallurgy* **30** (1992) 291.
2. C.A. Fleming, *Hydrometallurgy* **30** (1992) 127.
3. M.C. Jha, in *Proceedings of the First International Symposium on Precious Metals Recovery*, p XXI-1, Reno Nevada (1984).
4. V. Reyes, MSc thesis, Universidad Autónoma Metropolitana-Iztapalapa, México DF (1998).
5. D. Bennion and J. Newman, *J. Appl. Electrochem.* **2** (1972) 113.
6. F. Coeuret, *Electrochim. Acta* **21** (1976) 203.
7. F. Coeuret, D. Hutin and A. Gaunand, *J. Appl. Electrochem.* **6** (1976) 417.
8. J. Trainham and J. Newman, *J. Electrochem. Soc.* **124** (1977) 1528.
9. H. Olive and G. Lacoste, *Electrochim. Acta* **25** (1980) 1303.
10. F. Coeuret and A. Storck, *Information Chimique* **210** (1981) 121.
11. B. Waterman, F.A. Olson and T.N. Andersen, in: S. Srinivasan, R. Woods and P.E. Richardson (Eds), *Electrochemistry in Mineral and Metal Processing I*, PV 84-10, (Electrochemical Society Pennington, NJ, 1984), p. 611.
12. A. Stavart, C. Leroy and A. Van Lierde, *Minerals Eng.* **12** (1999) 545.
13. F.C. Walsh and W. Reade, in J.D. Genders and N.L. Weinberg (Eds), 'Electrochemistry for a Cleaner Environment' (Plenum, London, 1983), p. 393.
14. R.W. Houghton and A.T. Kuhn, *J. Appl. Electrochem.* **4** (1974) 173.
15. D. Genders and N. Weinberg, 'Electrochemistry for a Cleaner Environment' (Electrosynthesis, New York, 1992).
16. B. Fleet, in J.S. Stock and M.V. Orna (Eds), 'Electrochemistry Past and Present' (American Chemical Society, Oxford University Press, 1989), chapter 38.
17. D. Pletcher and F.C. Walsh, 'Industrial Electrochemistry' (Chapman & Hall, London, 2nd edn, 1990).
18. C. Ponce de León and D. Pletcher, *Electrochim. Acta* **4** (1996) 533.
19. G. Valentin and A. Storck, *J. Chim. Phys.* **85** (1988) 281.
20. H.E. Kreysa, 'Principles of Electrochemical Engineering' (VCH, New York, 1997).
21. G. Carreño Aguilera, MSc thesis, Universidad Autónoma Metropolitana-Iztapalapa, México DF (1996).
22. T.F. Otero and J.L. Rodríguez-Jiménez, *J. Appl. Electrochem.* **29** (1974) 239.

23. A. Ringbom, 'Complexation in Analytical Chemistry' (Wiley-Interscience, New York, 1963).
24. Y. Zhang, Z. Fang and M. Muhammed, *Hydrometallurgy* **46** (1997) 251.
25. S. Caroli and V.K. Sharma, 'Tables of Standard Electrode Potentials' (J. Wiley & Sons, New York, 1978).
26. A. Rojas, G. Trejo and M.T. Ramírez, 'Diagramas de Zonas de Predominio Aplicados al Análisis Químico', Universidad Autónoma Metropolitana-Iztapalapa, México DF (1993).
27. A. Rojas, M.T. Ramírez, J.G. Ibáñez and I. González, *J. Electrochem. Soc.* **138** (1991) 1921.
28. V. Reyes, M.T. Oropeza, I. González and C. Ponce de León, in M.T. Oropeza and I. González (Eds), Proceedings of XIV Meeting of Sibae, Oaxaca, México (2000), p. 18.
29. V.E. Reyes, M.T. Oropeza, I. González and C. Ponce de León, *Hydrometallurgy*, submitted.
30. S. Vilchis-Carbajal, I. González and G.T. Lapidus, *J. Appl. Electrochem.* **30** (2000) 217.
31. J. Li and M.E. Wadsworth, *J. Electrochem. Soc.* **140** (1993) 1921.
32. O.A. Ashiru and J.P.G. Farr, *J. Electrochem. Soc.* **139** (1992) 2806.
33. A.B. Soto, M.E. Palomar-Pardavé and I. González, *Electrochim. Acta* **41** (1996) 2647.
34. V.E. Reyes, M.T. Oropeza, I. González and C. Ponce de León, *Hydrometallurgy*, submitted.
35. O.A. Ashiru and J.P.G. Farr, *J. Electrochem. Soc.* **142** (1995) 3729.
36. E. Sosa, G. Carreño, C. Ponce de León, M.T. Oropeza, M. Morales, I. González, N. Batina, *Appl. Surf. Sci.* **153** (2000) 245.